Astronomy & Astrophysics manuscript no. article˙arxiv
December 23, 2011

© ESO 2011

arXiv:1112.5319v1 [astro-ph.GA] 22 Dec 2011

LETTER TO THE EDITOR

Chemical Differentiation toward the Pipe Nebula Starless Cores

P. Frau[1], J. M. Girart[1], and M. T. Beltrán[2]

[1] Institut de Ciències de l'Espai (CSIC-IEEC), Campus UAB, Facultat de Ciències, Torre C5p, 08193 Bellaterra, Catalunya, Spain
e-mail: `[frau;girart]@ice.cat`
[2] INAF-Osservatorio Astrofisico di Arcetri, Largo Enrico Fermi 5, 50125 Firenze, Italy
e-mail: `mbeltran@arcetri.astro.it`

Received 8 December 2011 / Accepted 22 December 2011

ABSTRACT

We used the new IRAM 30-m FTS backend to perform an unbiased ∼15 GHz wide survey at 3 mm toward the Pipe Nebula young diffuse starless cores. We found an unexpectedly rich chemistry. We propose a new observational classification based on the 3 mm molecular line emission normalized by the core visual extinction (A_V). Based on this classification, we report a clear differentiation in terms of chemical composition and of line emission properties, which served to define three molecular core groups. The "diffuse" cores, $A_V \lesssim 15$, show poor chemistry with mainly simple species (e.g. CS and C_2H). The "oxo-sulfurated" cores, $A_V \simeq 15$–22, appear to be abundant in species like SO and SO_2, but also in HCO, which seem to disappear at higher densities. Finally, the "deuterated" cores, $A_V \gtrsim 22$, show typical evolved chemistry prior to the onset of the star formation process, with nitrogenated and deuterated species, as well as carbon chain molecules. Based on these categories, one of the "diffuse" cores (Core 47) has the spectral line properties of the "oxo-sulfurated" ones, which suggests that it is a possible failed core.

Key words. ISM: individual objects: Pipe Nebula – ISM: lines and bands – ISM – stars: formation

1. Introduction

A new generation of sensitive receivers and wideband backends allows to study in detail the chemistry of faint starless cores. Several surveys have been performed toward them reporting a rich but relatively simple chemistry: essentially carbon chemistry with significant sulfur and nitrogen bearing molecules, followed by later deuteration which can be used as a chemical clock (e.g., Turner, 1994; Turner et al., 2000; Hirota & Yamamoto, 2006; Tafalla et al., 2006; Bergin & Tafalla, 2007). Recently, from the theoretical side, several papers have tried to model the starless core chemistry self-consistently (Aikawa et al., 2001; Garrod et al., 2005; Keto & Caselli, 2008).

The Pipe Nebula is a nearby (145 pc: Alves & Franco, 2007) cloud that harbors more than one hundred of low mass (∼1 $M_\odot$) starless cores, most of them gravitational unbound but confined by the thermal/magnetic pressure of the whole cloud (Alves et al., 2008; Lada et al., 2008; Franco et al., 2010). The Pipe Nebula differs from the other nearest dark cloud complexes such as Taurus or ρ Ophiuchus because it has a very small star formation efficiency (Onishi et al., 1999; Forbrich et al., 2009; Román-Zúñiga et al., 2010, 2011). Thus, the Pipe Nebula is an ideal target to study the physical and chemical conditions in a pristine environment prior to the onset of the star formation process, as the recent numerous studies have shown (e.g., Brooke et al., 2007; Muench et al., 2007; Rathborne et al., 2008). Frau et al. (2010) present the first results of an extensive continuum and molecular line study on a subset of a selected sample of cores distributed in the different regions of the Pipe Nebula: *bowl*, *stem*, and B59. The cores are in general less dense and less chemically evolved than starless cores in other star forming regions studied (e.g. Crapsi et al., 2005). We find very different morphologies and densities, and no clear correlation of the chemical evolutionary stage of the cores with their location in the cloud. The Pipe Nebula starless cores have shown to be more heterogeneous than expected.

In this work, we present a wide (∼15 GHz) unbiased chemical survey at 3 mm toward a larger sample of Pipe Nebula starless cores, spanning a factor of 6 in their visual extinction (A_V) peaks. This is a first step to characterize their varied chemistry in order to proceed to future modeling.

2. FTS Observations and Data Reduction

We made pointed observations toward the Pipe Nebula Cores 06, 08, 12, 14, 20, 33, 40, 47, 48, 56, 65, 87, 102 and 109, following Rathborne et al. (2008) numbering, and toward a position with no cores. We pointed either toward the continuum emission peak (Frau et al., 2010, 2011), if available, or toward the $C^{18}O$ pointing center reported by Muench et al. (2007). We assumed that the pointing centers were the densest region of the cores and, therefore, with the richest chemistry. We used the EMIR heterodyne receiver of the IRAM 30-m telescope tuned at the C_2H (1–0) transition (87.3169 GHz). At this frequency the telescope delivers θ_{HPBW}=28.″1, $B_{\rm eff}$=0.81 and $F_{\rm eff}$=0.95. The observations were carried out in August 2011, being the first astrophysicists to use the FTS autocorrelator as the spectral backend. We selected a channel resolution of 195 kHz (≃0.6 km s^{-1}at 3 mm) which provided a total bandwidth of 14.86 GHz covering the frequency ranges from 82.01 to 89.44 GHz, and from 97.69 to 105.12 GHz. We used the frequency-switching mode with a frequency throw of 7.5 MHz. System temperatures ranged from ∼110 to ∼150 K. Pointing was checked every 2 hours. We reduced the data using the CLASS package of the GILDAS[1] software. The baseline in the frequency switching mode for such a

---

[1] available at http://www.iram.fr/IRAMFR/GILDAS

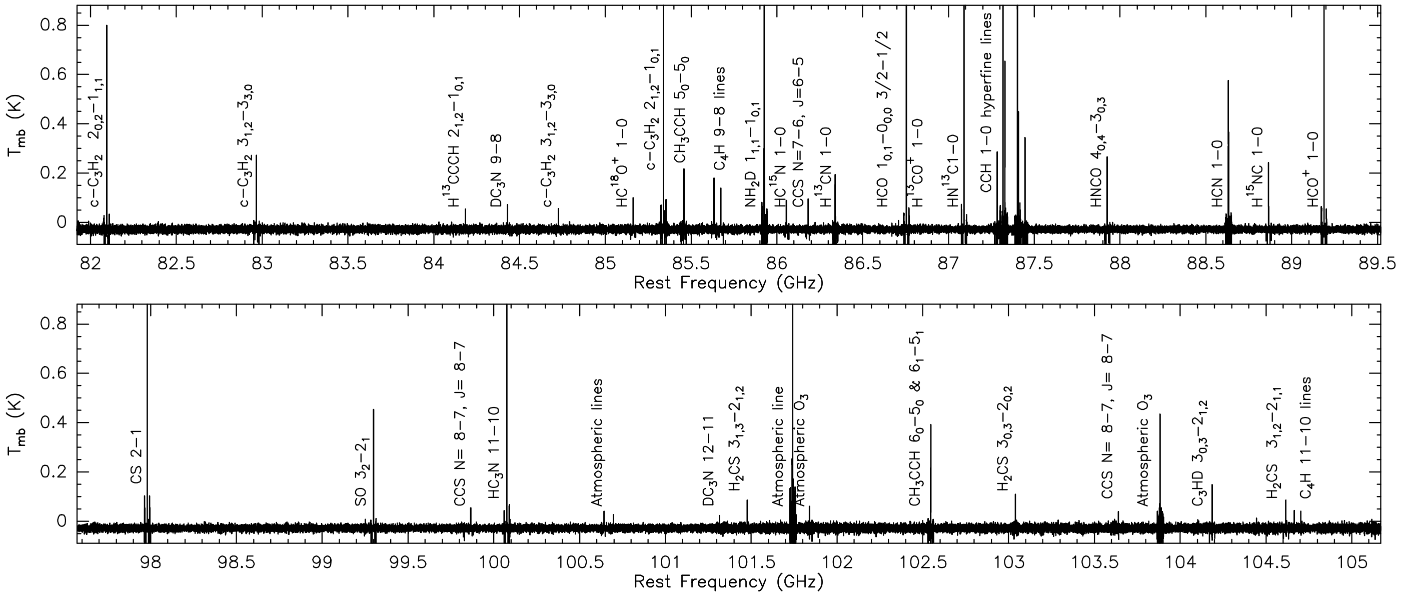

Fig. 1. IRAM 30-m EMIR+FTS full bandwidth spectrum toward Core 12. The most important detected molecular transitions are labeled within the plot. The upper and lower panels show the ~7.6 GHz lower and upper sidebands, respectively. The noise rarely exceeds 10 mK. The negative emission are the twin negative counterparts of the positive emission due to the frequency-switching observing mode.

large bandwidth (~3.7 GHz for each chunk) has a complicated shape with sinusoidal-like ripples. Nevertheless, since the observed lines are very narrow ($\lesssim$0.5 km s^{-1}, similar to the effective spectral resolution), the baselines can be efficiently removed if small windows are used ($\lesssim$20 MHz). The resulting typical rms noise was $\simeq$8 mK at the 195 kHz spectral resolution.

3. Results

The large available bandwidth, 14.86 GHz, has allowed us to carry out an unbiased survey, covering about a third of the observable 3 mm window. We used the *Splatalogue*[2] tool to identify possible lines. We consider tentative detections those lines with intensities in the 3–5σ range, and fiducial detections those higher than 5σ. We have detected 53 transitions from a total of 31 molecules (including isotopologues). Figure 1 shows the observed bandwidth toward Core 12 with the main molecular species labeled. Most of the detected lines were identified in this core, the one with the highest A_V and the brightest molecular line emission of the sample. However, there are few sulfur bearing molecular lines not detected toward Core 12 but present in other cores: SO_2 $3_{1,3}$–$2_{0,2}$, ^{34}SO 3_2–2_1, and OCS 7–6. We report tentative detections (~4σ) of $HOCO^+$ (Cores 6 and 102), l-C_3H (Cores 12 and 109), and HCCNC (Core 12). We have also identified in all the cores several Earth atmospheric lines, mostly from ozone.

The cores with the brightest detected lines are those with highest A_V (Cores 12, 87 and 109) due to their larger gas column densities. In order to avoid a column density bias (our core sample spans a factor of 6 in A_V), we have normalized the intensity by dividing the spectra by the A_V peak of the core. We used the values obtained by Román-Zúñiga et al. (2010) from dust extinction maps that have an angular resolution similar to our observations. This definition mimics molecular abundances for optically thin lines. Figure 2 shows a selected sample of the brightest normalized lines toward all the sample, with the cores ordered by their A_V peak. In this figure we have ordered the molecules in families taking into account their atomic composition.

In general, the 3 mm transitions of the lightest species of most of the molecular families (blue spectra in Fig. 2) were detected in all the cores of our sample: C_2H, HCO^+, CS, SO, and HCN. c–C_3H_2 can also be part of this sample, since it was detected in all but two cores. The 3 mm main transitions of these molecules can be considered "ubiquitous lines" in starless cores. HCO^+ 1–0, CS 2–1, and HCN 1–0 show little variations in normalized intensity. These molecules have large dipole moments and high abundances, therefore they likely have large optical depths (Frau et al., 2011). In addition, the HCO^+ 1–0 and HCN 1–0 transitions can be affected by absorption by low density foreground gas (Girart et al., 2000). Indeed, the relative HCN 1-0 hyperfine line intensities of Cores 12, 40 and 87 suggest that this transition is out of LTE. The normalized intensities of the other three ubiquitous lines show significant variations within the sample. However, while C_2H 1–0 and c–C_3H_2 $2_{1,2}$–$1_{0,1}$ tend to increase with A_V, the SO 3_2–2_1 line appears to have the largest normalized intensities in the cores with visual extinction in the range of 15 to 22 mag.

Several molecular transitions were detected only toward cores with $A_V \gtrsim 15$. The optically thin $H^{13}CO^+$ 1–0, and $HC^{18}O^+$ 1–0, and the transition HNCO $4_{0,4}$–$3_{0,3}$, show larger normalized intensities with increasing column densities. The detected transitions from oxo-sulfurated molecules (SO 2_2–1_1, ^{34}SO 3_2–2_1, SO_2 $3_{1,3}$–$2_{0,2}$ and OCS 7–6) are mainly detected toward the cores with the brightest SO 3_2–2_1 emission, this is, mainly in the cores with $A_V \simeq 15$–22 mag. The HCO 1–0 transition shows the same behavior. Curiously and despite its low density (A_V=11.2 mag), Core 47 shows emission in most of the oxo-sulfurated molecular transitions as well as in HCO 1–0. The H_2CS $3_{1,3}$–$2_{1,2}$ transition appears to show a similar trend to the oxo-sulfurated molecules, although it peaks at slightly denser cores ($A_V \simeq 20$ mag) and clearly survives at larger A_V values. The emission of the other two lines of this group, HCS^+ 2–1 and $^{13}C^{18}O$ 1–0, is too weak to show a clear trend.

---

[2] http://www.splatalogue.net/

The number of detected molecular transitions increased significantly for the four cores with the highest column density ($A_V \gtrsim 22$ mag) due to either (*i*) excitation/column density reasons or (*ii*) synthesization timescales. The c–C_3H_2 molecule is a good example of the former molecules. Although being ubiquitous in the $2_{1,2}$–$1_{0,1}$ transition, the $3_{1,2}$–$3_{0,3}$ one is only detected at these column densities. The rarer isotopologic counterparts of the HCN and c–C_3H_2 1–0 ubiquitous lines ($H^{13}CN$, $HC^{15}N$, and c–$H^{13}CCCH$) are detected only in these four cores. This is also the case for $HN^{13}C$ and $H^{15}NC$ in the 1–0 transition, which suggests that the HNC 1–0 is likely to be an ubiquitous line as well. Most of the transitions detected in these four cores show larger normalized intensities with increasing A_V (e.g. HC_3N 11-10). The carbon-chain molecular transitions (C_4H 9–8 and 11–10, and CH_3C_2H 5_n–4_n and 6_n–5_n) are the exception, showing little variations in normalized intensity. Several transitions of three deuterated forms of abundant species were also detected: C_3HD $3_{0,3}$–$2_{1,2}$, NH_2D 1-1, and DC_3N in the 9–8 and 12-11 (see Fig. 2). Only the first transition is detected in the four cores.

4. Discussion and Conclusions

The chemistry detected toward the sample of fourteen starless cores is unexpectedly rich taking into account their low temperatures (10–15 K: Rathborne et al., 2008) and visual extinctions. The apparent correlation within the sample of the 3 mm molecular transition normalized intensities to visual extinction allow us to propose an observational classification (see Fig. 2). We define three groups of starless cores, which are probably related with their dynamical age: *"diffuse"*, *"oxo-sulfurated"*, and *"deuterated"* cores. This classification can be useful in future wide band 3 mm observations of molecular clouds.

– *"Diffuse" cores*: a set of cores with small column densities ($A_V \lesssim 15$ mag $\sim N_{H_2} \lesssim 1.2 \times 10^{22}$ cm^{-2}) lies above the blue dot-dashed horizontal line in Fig. 2. Their spectra is rather poor, showing only significant normalized intensity in the transitions of the main isotopologues of abundant species like C_2H, HCN (and likely HNC), HCO^+ and SO. Such a simple observational chemistry suggests that these are very young starless cores, or even transient clumps on which essentially the cloud chemistry is better detected due to density enhancements. Core 47 is a clear exception and it is discussed later in the text.

– *"Oxo-sulfurated" cores*: a group of denser cores ($A_V \simeq 15$–22 mag $\sim N_{H_2} \simeq 1.2 \times 10^{22}$–$1.7 \times 10^{22}$ cm^{-2}) that show richer chemistry but not yet significant deuteration to be observed. In Fig. 2 this group lie between the blue dot-dashed and red dashed horizontal lines. All the transitions detected in the *"diffuse"* cores are also present. The SO 3_2–2_1 transition is the main signpost as it is very bright. Many other oxo-sulfurated molecules (^{34}SO, SO_2, and OCS), as well as HCO, exhibit a same trend, but they are not detected at higher densities. This suggests an increase of these chemically related species in the gas-phase in this A_V range, followed by a later depletion/destruction as density increases. These cores might be in-the-making cores, which have developed a richer chemistry and piled up more material, probably in a stage near to the onset of collapse (Ruffle et al., 1999). Core 102 is an exception in this group and is discussed later in the text.

– *"Deuterated" cores*: the densest cores of the sample ($A_V \gtrsim 22$ mag $\sim N_{H_2} \gtrsim 1.7 \times 10^{22}$ cm^{-2}), shown below the red dashed horizontal line in Fig. 2. Core 12, the densest one, sets the upper limit at A_V=67.2 mag ($N_{H_2} \simeq 5.3 \times 10^{22}$ cm^{-2}). These cores are generally bright in the transitions typical of the other two groups. The oxo-sulfurated molecules are the exception, hardly present, probably depleted/destructed at the densities reached. The main signpost are the emission, only present in this group, in rare isotopologues of the nitrogenated ubiquitous lines ($H^{13}CN$, $HC^{15}N$, $HN^{13}C$, and $H^{15}NC$), deuterated forms of abundant species (C_3HD, NH_2D, and DC_3N), and carbon-chain molecules (C_4H and CH_3C_2H). These cores might be stable starless cores with a life-time long enough to achieve the densities needed to synthesize efficiently carbon chains and deuterated species (Roberts & Millar, 2000; Gwenlan et al., 2000).

As already said, Core 47 does not match the chemical properties of the diffuse cores. It shows a chemistry matching the oxo-sulfurated group, which proved to be very sensitive to density. This suggests that it might be a failed core which developed a rich chemistry and is now merging back into the cloud. This scenario can increase the oxo-sulfurated chemistry detected (Garrod et al., 2005). Core 47 is located close to Core 48 in the only Pipe Nebula region with superalfvénic turbulence, as shown by optical polarization observations (Franco et al., 2010). Therefore, it is possible that an external source of turbulence is disrupting the medium in this area and dispersing the cores.

On the other hand, Core 102, in the oxo-sulfurated group, shows a chemistry similar to that of the diffuse cores. Similarly, Core 87, among the deuterated cores, shows features of the oxo-sulfurated group. This suggests that these cores might have piled up material so quickly that a more complex chemistry had no time to be synthesized. Both cores lie in the same N-S oriented high-density structure (Román-Zúñiga et al., 2010) where Franco et al. (2010) report a N-S magnetic field. The fast evolution might have been driven by magnetic fields with the surrounding mass collapsing in this direction.

The FTS chemical survey toward the starless cores of the Pipe Nebula showed a chemistry much more rich than expected for a cloud giving birth to low-mass stars at very low efficiency. A good interpretation of the results demands chemical modeling to investigate a possible evolutive track, which will be the purpose of a forthcoming study.

Acknowledgements. PF is partially supported by MICINN fellowship FPU (Spain). PF, JMG and MTB are supported by MICINN grant AYA2008-06189-C03 (Spain). PF, JMG and MTB are also supported by AGAUR grant 2009SGR1172 (Catalonia). We thank Carlos Román-Zúñiga for gently sharing the A_V maps. The authors want to acknowledge all the IRAM 30-m staff for their hospitality during the observing runs, the operators, and the AoDs for their active support. We thank the anonymous referee for useful comments. This research has made use of NASA's Astrophysics Data System.

References

Aikawa, Y., Ohashi, N., Inutsuka, S.-i., Herbst, E., & Takakuwa, S. 2001, ApJ, 552, 639
Alves, F. O. & Franco, G. A. P. 2007, A&A, 470, 597
Alves, F. O., Franco, G. A. P., & Girart, J. M. 2008, A&A, 486, L13
Bergin, E. A., & Tafalla, M. 2007, ARA&A, 45, 339
Brooke, T., Huard, T. L., Bourke, T. L., Boogert, A. C. A. et al. 2007, ApJ, 655, 364
Crapsi, A., Caselli, P., Walmsley, C. M., et al. 2005, ApJ, 619, 379
Forbrich, J., Lada, C. J., Muench, A. A., Alves, J., Lombardi, M. 2009, ApJ, 704, 292
Franco, G. A. P., Alves, F. O., & Girart, J. M. 2010, ApJ, 723, 146
Frau, P., Girart, J. M., Beltrán, M. T., et al. 2010, ApJ, 723, 1665
Frau, P., Girart, J. M., Beltrán, M. T., et al. 2011, in preparation
Garrod, R. T., Williams, D. A., Hartquist, T. W., Rawlings, J. M. C., & Viti, S. 2005, MNRAS, 356, 654
Girart, J. M., Estalella, R., Ho, P. T. P., & Rudolph, A. L. 2000, ApJ, 539, 763
Gwenlan, C., Ruffle, D. P., Viti, S., Hartquist, T. W., & Williams, D. A. 2000, A&A, 354, 1127
Hirota, T., & Yamamoto, S. 2006, ApJ, 646, 258

Keto, E., & Caselli, P. 2008, ApJ, 683, 238
Lada, C. J., Muench, A. A., Rathborne, J. M., Alves, J. F., & Lombardi, M. 2008, ApJ, 672, 410
Muench, A. A., Lada, C. J., Rathborne, J. M., Alves, J. F., & Lombardi, M. 2007, ApJ, 671, 1820
Onishi, T., Kawamura, A., Abe, R., Yamaguchi, N. et al. 1999, PASJ, 51, 871
Rathborne, J. M., Lada, C. J., Muench, A. A., Alves, J. F., & Lombardi, M. 2008, ApJS, 174, 396
Roberts, H., & Millar, T. J. 2000, A&A, 361, 388
Román-Zúñiga, C., Alves, J. F., Lada, C. J., & Lombardi, M. 2010, ApJ, 725, 2232
Román-Zúñiga, C., Frau, P., Girart, J. M., & Alves, J. F. 2011, ApJL, submitted
Ruffle, D. P., Hartquist, T. W., Caselli, P., & Williams, D. A. 1999, MNRAS, 306, 691
Tafalla, M., Santiago-García, J., Myers, P. C., et al. 2006, A&A, 455, 577
Turner, B. E. 1994, ApJ, 420, 661
Turner, B. E., Herbst, E., & Terzieva, R. 2000, ApJS, 126, 427

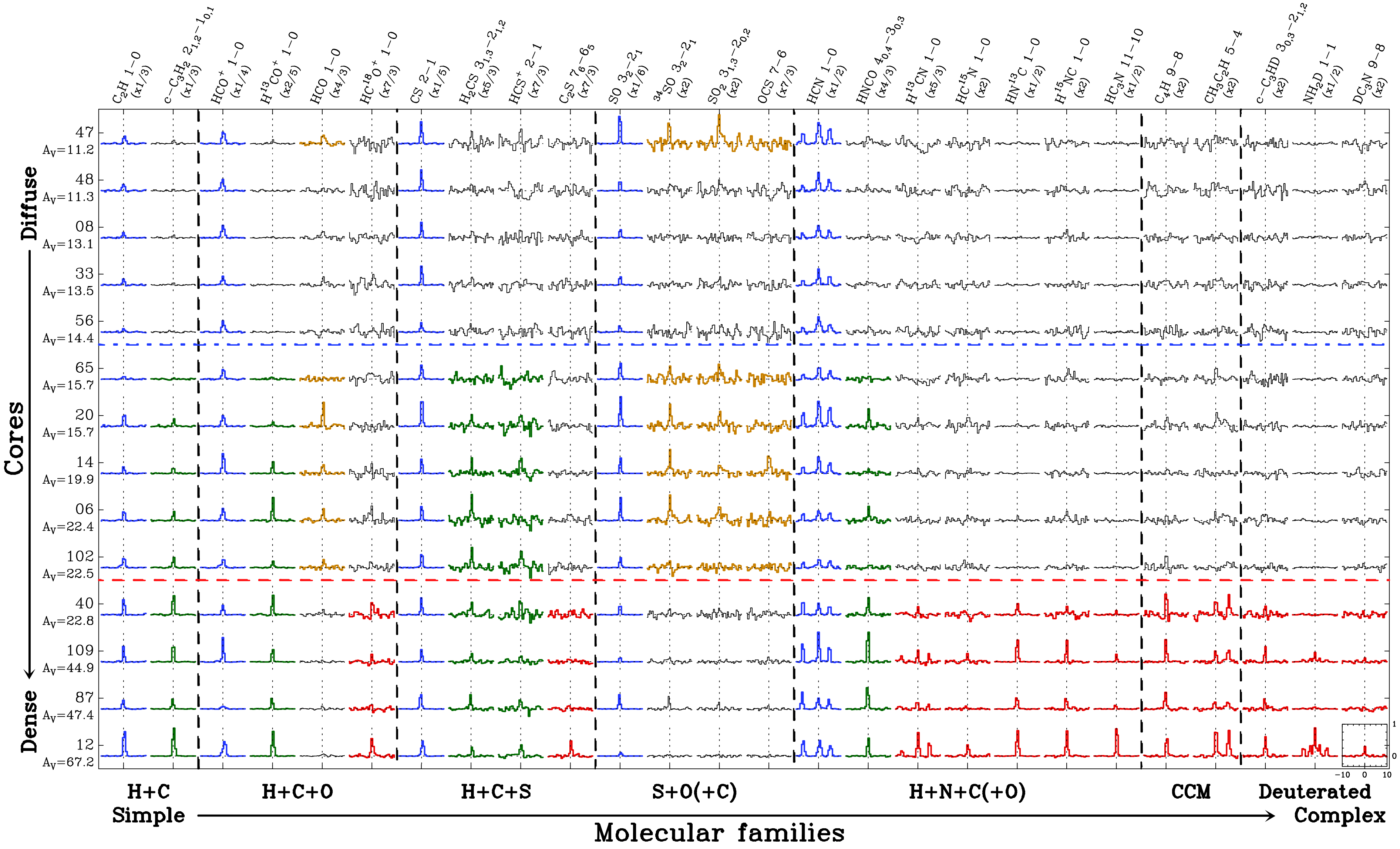

Fig. 2. Selected normalized molecular transitions toward the observed cores. The scale is shown in the bottom right spectrum. The normalized intensity axis ranges from -0.33 to 1, while the velocity axis spans 20 km s^{-1} centered at the v$_{\rm LSR}$. *Rows*: individual cores, labeled on the left-hand side of the figure, ordered by its A_V peak. *Columns*: molecular transition, ordered by molecular families, labeled on the top of the figure. The spectra have been divided by [A_V/100 mag] to mimic the abundance, where the A_V value is that at the respective core center (Román-Zúñiga et al., 2010) given below the core name. Each molecular transition has been multiplied by a factor, given below its name, to fit in a common scale. *Colors*: used to highlight the distinctive emission of the different core groups. blue: ubiquitous lines, green: dense-medium molecular transitions, orange: molecular transitions typical in oxo-sulfurated cores (see Sect. 4), red: molecular transitions typical in deuterated cores, and **black**: mostly undetected species.